Construction and Building Materials 156 (2017) 402–411

Contents lists available at ScienceDirect

Construction and Building Materials

journal homepage: www.elsevier.com/locate/conbuildmat

Experimental and numerical study on mechanical properties of Ultra High Performance Concrete (UHPC)

Mohamadreza Shafieifar *, Mahsa Farzad, Atorod Azizinamini

Department of Civil and Environmental Engineering, Florida International University, FL, United States

HIGHLIGHTS

- A series of compression and tensile tests for UHPC and Normal strength concrete was carried out.
- The module elasticity and average compression and tensile strength of the materials were evaluated.
- A calibrated Finite Element model using Concrete Damage Plasticity (CDP) was developed to predict the behavior of the UHPC.
- Experimental and numerical results were compared and the effects of the mesh sizes were discussed.

ARTICLE INFO

Article history:
Received 5 June 2017
Received in revised form 21 August 2017
Accepted 30 August 2017
Available online 9 September 2017

Keywords:
UHPC
Compression and tensile stress strain
Concrete plasticity damage
CDP
Abaqus
Modulus of elasticity

ABSTRACT

Ultra-High Performance Concrete (UHPC) is an advanced technology in concrete industry with superior characteristics such as high strength in compression and tension, ductility, and durability. This paper determines the tensile and compressive behavior of UHPC and a comparison is made with Normal Strength Concrete (NC) for the development of a numerical model to simulate the behavior of UHPC using the Finite Element (FE). The experimental tests including a cylinder and cube compressive test, flexural, briquette and splitting tension tests to evaluate the ultimate capacity of the material in compression and tension and its modulus of elasticity. The primary focus of this research, however, was to simulate material properties of UHPC through commercial FE software allowing the study of the structures including UHPC. The numerical analysis provides the mechanical properties of UHPC that can be used in FE software using Concrete Damage Plasticity model (CDP) to define ductal UHPC in the absence of sufficient experimental data. The numerical and the experimental results were generally in good agreement.

1. Introduction

Although concrete is the most universally used material in building there are still some limitations to its use, such as low tensile strength and brittleness. Ultra-High Performance Concrete (UHPC), a cutting-edge concrete, may be able to overcome these concerns. As the Federal Highway Administration (FHWA) reports: UHPC is a cementitious material formulated by mixing Portland cement, fine silica sand, silica fume, quartz flour, high-range water reducer, discontinuous internal steel or organic fibers, and less than 0.25 water-to-cement (W/C) ratio. UHPC offers more than 21.7 ksi (150 Mpa) compressive strength and greater than 0.72 ksi (5 Mpa) sustained post-cracking tensile strength [1]. The discontinuous pore structure of UHPC reduces liquid ingress and significantly enhances durability compared to conventional concrete [2].

This report determines the basic mechanical properties of UHPC and normal strength concrete (NC) to make an apple-to-apple comparison and to develop a numerical model to simulate the behavior of UHPC using the finite element (FE). The experimental tests done on the materials include cylinder and cube compressive strength tests, as well as flexural strength, briquette tensile, and splitting tension tests. The major focus of this research, however, was to simulate UHPC material through commercial FE software allowing the study of the structures including UHPC. To that aim, a three-dimensional FEM simulation in Abaqus has been used to model the failure process of the experimentally tested compression cylinders and cubes along with flexural prisms.

Ductal®, an available commercial product, was the UHPC product used in this study, which is a product of Lafarge, Inc. composed of premix powder, water, superplasticizer, and metallic fibers (2% in volume).

* Corresponding author at: 10555 West Flagler Street, EC1234, Miami, FL 33174, United States.
E-mail address: mshaf017@fiu.edu (M. Shafieifar).

http://dx.doi.org/10.1016/j.conbuildmat.2017.08.170
0950-0618/

2. Literature review

UHPC possesses a compressive strength greater than 21.7 ksi (150 Mpa) and a flexural strength greater than 0.72 ksi (10 Mpa) at 28 days. The concept of UHPC was first developed by Richard and Cheyrezy and was produced in the early 1990s at Bouygues Laboratory in France [3]. Afterward, the effect of fiber addition on the improved ductile behavior of beams was investigated by Oh [4] and Ashour et al. [5]. Moreover, the increased bearing capacity and shear strength of fiber-reinforced beams were studied by Campione [6], and by Lim et al. [7] respectively.

The mechanical properties of both plain and fiber reinforced UHPC mixtures, proportioned using commercially available materials, were investigated by Wille et al. [8]. In his research, in addition to silica fume and fine sand, silica powder (glass powder) was used to increase reactivity. The highest compressive strength of $2 \times 2 \times 4$ in. ($50 \times 50 \times 100$ mm) size cubes, under moist curing conditions at 20 °C, was 29 ksi (201 Mpa) for steel fiber reinforced UHPC, and 27.8 ksi (192 Mpa) for plain UHPC. They also tested $4 \times 4 \times 16$ in. ($100 \times 100 \times 400$ mm) prisms to measure the flexural strength and the highest flexural strength was reported as 2 ksi (13.95 Mpa) for fiber reinforced and 1.1 ksi (7.5 Mpa) for plain UHPC. They also observed that the specimens without fibers failed in flexure immediately after the first crack, demonstrating the influence of fibers on the ductility of UHPC.

Allena and Newtson [9] reported that the greatest compressive strength obtained from 2 in. (50 mm) and 4-in. (100 mm) cubes were 24.7 ksi (170.3 Mpa), and 21.7 ksi (149.5 Mpa) respectively. These numbers for plain UHPC were also reported as 23.2 ksi (159.9 Mpa) and 20.5 ksi (141.2 Mpa), approximately 6% lower than compressive strengths of fiber reinforced UHPC. They also considered the flexural strength of UHPC specimens using ($75 \times 100 \times 400$ mm) prismatic specimens and reported the greatest flexural strength as 2.65 ksi (18.3 Mpa) for fiber reinforced UHPC and 1.6 ksi (10.9 Mpa) for plain UHPC.

The mechanical properties of UHPC and High-Performance Concrete (HPC) were studied by Dili and Santhanam [10]. 2-in. (50 mm) cubes were wet cured at 90 °C and tested to measure the compressive strength. The maximum compressive strength observed for UHPC was 29 ksi (200 Mpa). Moreover, they investigated the flexural behavior of $1.6 \times 1.6 \times 6.4$ in. ($40 \times 40 \times 160$ mm) prisms including both plain and fiber reinforced UHPC. In the research, the flexural strength of fiber reinforced UHPC and HPC prisms were reported greater than the flexural strength of the plain prisms. However, the flexural strength of UHPC prisms was observed considerably greater than that of HPC prisms.

Graybeal [11,12] did numerous investigations of the mechanical properties of Ductal. In his study, the compressive strength of Ductal UHPC was tested using 2×4 in. (50×100 mm), 3×6 in. (75×150 mm), and 4×8 in. (100×200 mm) cylinders as well as 2×4 in. (50×100 mm) cube specimens. He reported a compressive strength of 28 ksi (193 Mpa) from 3×6 in. (75×150 mm) cylinders and the average split tensile strength of UHPC cylinders 4×8 in. (100×200 mm) of 1.6 ksi (10.9 Mpa). There are several publications regarding the recent researches on UHPC [13,14].

This research includes two phases, one experimental and one numerical. The experimental phase focuses on determining the basic material properties from small-scale testing of UHPC and NC including the test of over 66 individual specimens (33 specimens UHPC and 33 specimens NC), with an emphasis toward determining the compressive and tensile behaviors. In this phase, the material characterization is completed according to ASTM standard procedures [15]. The test results from this study provide more information to help establish a prediction model for UHPC elements under various loading conditions, which form the future studies.

The first step of each project is to numerically analyze the behavior of the structure for which the defined material property plays the most crucial role. The main goal of the numerical part of the research is to provide a simple numerical calibrated model of one of the commercially available UHPCs (Ductal). This model will help researchers to simulate UHPC material. To that aim, the results obtained from compression cylinders and cubes, as well as flexural prisms, were used to simulate UHPC behavior in FE software. The other specimens were not included in the numerical analysis due to their unknown boundary condition.

3. Experimental study

3.1. Material mixing

Among the advanced concrete technology [16] UHPC receiving universal attention. Three parts of the UHPC used in this study included: premix, fibers, and liquids. The premix (Ductal® JS1000) contains all of the cementitious, aggregate, and filler materials provided by Lafarge®. UHPC, compared to conventional concrete, shows remarkably improved mechanical properties such as high compressive strength, high tensile strength, and high workability. The premix was batched by the manufacturer and delivered to FIU's Structural Lab. Its composition is given in Table 1.

The liquids mixed with the UHPC included water, in the form of ice, and Superplasticizer as a high-range water-reducing admixture (HRWA). The W/C ratio of all batches was 0.15 and straight steel fibers having circular cross sections with a diameter of 0.008 in. (0.2 mm) and length of 0.5 in. (12.5 mm). The tensile strength of these fibers was specified with a minimum of 377 ksi (2600 Mpa) by the manufacturer. The concentration of 2% by volume of fibers were included in the mix.

To obtain a consistent performance, a strict mixing procedure was followed, in which materials were weighed and placed in a nine ft^3 capacity mortar mixer. The premix was initially dry mixed for nearly 4 min. Then half of the superplasticiser and ice (water) were added to the mix and mixed for an additional 15 min. The remaining superplasticizer was then added, and the materials were mixed until the dry powder mix transformed into a wet paste concrete (approximately 2 min). Steel fibers were slowly added by hand to the wet concrete paste in the mixer. Since fiber addition has a strong impact

Table 1
Composition of Ductal®.

Premix	Material	lb/ft^3	kg/m^3	Percentage by Weight
	Portland Cement	44.4	712	28.5
	Fine Sand	63.7	1020	40.8
	Silica Fume	17.4	231	9.3
	Ground Quartz	13.1	211	8.4
	Accelerator	1.9	30	1.2
	Total Premix	140.5	2204	88.2
Superplasticizer		1.9	30.7	1.2
Steel Fiber		9.7	156	6.2
Water		6.8	109	4.4

Fig. 1. All UHPC specimens.

on the fiber distribution, this process was carried out carefully. The concrete was mixed for a further 6 min to ensure proper distribution of fibers, and then the UHPC was ready to be cast.

As soon as mixing was completed, the casting started. The casting of all UHPC specimens was completed within 15 min after completion of mixing. The UHPC was scooped into the molds and was not rodded due to the presence of the fibers. The exposed surfaces of each specimen were then covered in plastic to prevent moisture loss.

The NC used in the study was provided by a local supplier as a ready mix with a nominal strength of 5000 psi, and a slump of 4 in. (100 mm). The compacting procedure for NC specimens was done according to ASTM specification (ASTM C31-69) [15].

The demolding of all specimens occurred approximately 24 h after casting. The curing treatment applied to all specimens for this research was wet curing for 27 days starting from the demolding day, and then the specimens were tested (Fig. 1).

3.2. Test procedures and results

A universal testing machine (UTM) with a maximum capacity of 500 Kips and a 50-kip capacity MTS testing machine was used to apply a load to the specimens. Also, for all specimens, two potentiometers were placed to measure displacement. The collection of the data for all tests was completed through a data acquisition system set to record data at 10 Hz. The time, load, deflection values were all recorded. Density of UHPC and regular concrete were 155 lb/ft^3 (2480 kg/m^3) and 150 lb/ft^3 (2400 kg/m^3) respectively.

3.2.1. Compression testing

One of the most commonly specified and measured properties of concrete is compression strength. The modulus of elasticity, which is similarly measured through standardized compression test methods, is also regularly engaged parameter in the design of structures. All the compression tests discussed in this section were all completed nominally according to the ASTM C39 [15] standard test method for cylinders and the ASTM C109 [15] standard test method for cubes.

3.2.1.1. Cylinder tests. Uniaxial compression tests were performed on a total of 5 UHPC and 5 NC cylindrical specimens of 3 in.- (75 mm) diameter and 6 in.- (150 mm) tall cast in a plastic mold using ASTM C 39 guideline [15].

Prior to each test, all the cylinder specimens were grinded to minimize uneven surfaces at each end. The cylinders were measured to determine length, diameter, and density. Loading was applied at the rate of 440 lb/s; however, based on a study done by Graybeal [11] an increase in the load rate on compression testing results, would not be detrimental. Fig. 2 shows a picture of typical UHPC and NC cylinders after testing. In this figure it is noticeable that with the presence of fiber in the case of UHPC, the cylinder remains intact after failure.

The stress-strain curve of UHPC and NC, which is shown in Fig. 3, was obtained based on the load-displacement relationship, and the compressive strength and elastic modulus were calculated. Due to the difference between the stress-strain curve of UHPC and that of conventional concrete, the FHWA [11] suggests calculating the elastic modulus using values that correspond to 10% and 30% of the ultimate compressive strength. The average result of the test is listed in Table 2.

The NC specimens behave elastically up to the peak strength followed by a rapid strain softening. After the formation of the first crack, when lateral deformation surpassed its tensile capacity, the NC specimens lost their total strength and failed in a sudden explosive manner, see Fig. 3(b). In contrast, UHPC specimens behave elastically until approximately 50% of their compressive strength, followed by strain hardening behavior up to peak strength. The interaction between the fibers and the matrix resulted in ductile compressive failure where the concrete surface remains intact even at total strength loss; see Fig. 3(a). As illustrated in the results, no descending branch in the case of NC is observed which indicates the brittle behavior of the material, while in UHPC descending branch of the stress-strain curve is observed (Fig. 4).

3.2.1.2. Cube tests. At the same time as the cylinder tests, 2- and 3-in. (50 and 75 mm) cube specimens were also tested to measure compressive strength according to ASTM C109 [15] standard test method. Generally, the cylinder compressive strength is lower than its cube strength for the same concrete. This is due to the confining effect of the testing machine platens and the aspect ratio of the specimen. A strength reduction factor used to convert the cube strengths to cylinder strengths is usually in the vicinity of 0.82

Fig. 2. Cylinders after test: a) UHPC cylinders, and b) NC cylinders.

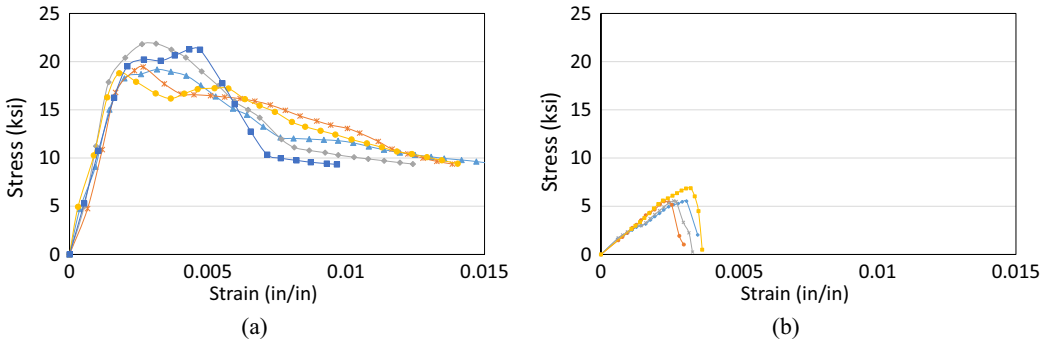

Fig. 3. The stress-strain curve based on cylinder test of the specimens: a) UHPC, and b) NC.

Table 2
Compressive cylinder test results.

Test	UHPC	NC
Compressive cylinder test	20.1 ksi (138 Mpa)	5.86 ksi (40.4 Mpa)
Modulus of elasticity	8700 ksi (60 Gpa)	3200 ksi (22.06 Gpa)

for normal concrete and increases toward 1.0 as the concrete strength increases [5].

The load rate for 2-in. (50 mm) and 3-in. (75 mm) cube compression tests were set at 200 lb/s and 675 lb/s respectively. In order to keep the test results consistent, uneven loading surfaces were minimized by applying the load on the vertical molded faces. The average result of the test is listed in Table 3.

The compressive stress-strain curve for both materials obtained from cubic tests is shown in Fig. 5.

3.2.2. Tensile behavior

Even though concrete is not typically designed to resist direct tension, and tensile strength constitute in normal strength concrete in building design is almost ignored, tensile strength is used to estimate the load under which cracking will happen. In contrast, the tensile strength of UHPC is much higher than that of NC, meaning that it can sustain tensile strength after the occurrence of the first crack. Consequently, determination of tensile strength of UHPC plays a major role in design.

In this investigation, three test methods were used to determine the tensile strength of concrete including flexural test, direct tensile test, and splitting tension.

3.2.2.1. Flexural test. The ASTM C1018 [15] Standard test method for flexural toughness was one test used to determine the tensile properties of UHPC and NC. Prisms of $20 \times 6 \times 6$ in.

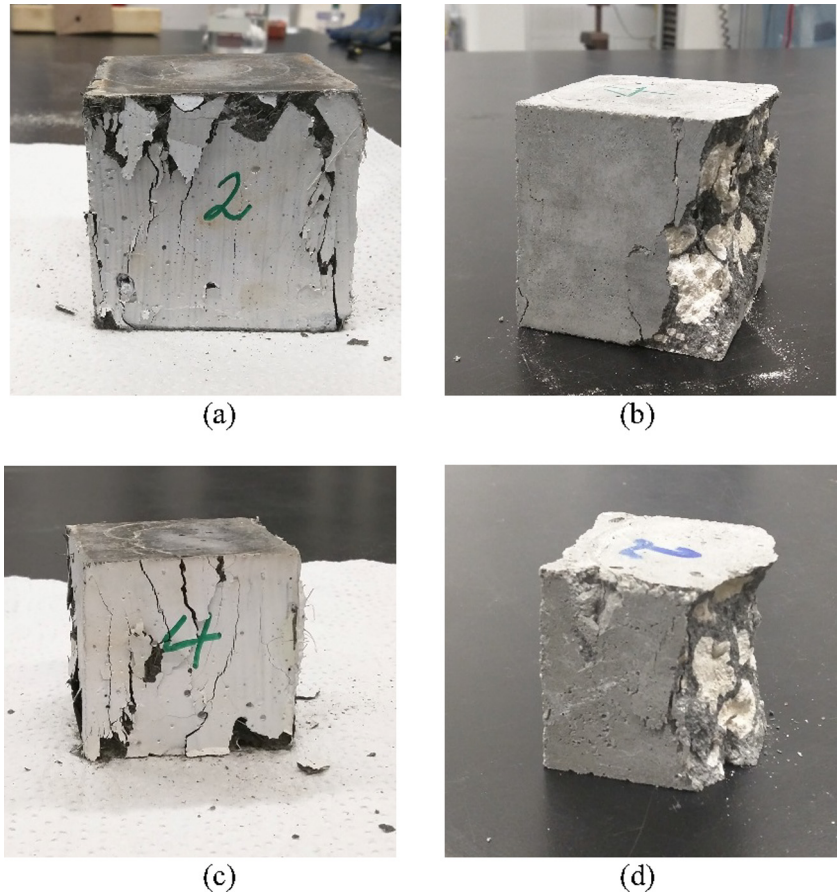

Fig. 4. a) 3-in. (75 mm) UHPC cube, b) 3-in. (75 mm) NC cube, c) 2-in. (50 mm) UHPC cube, and d) 2-in. (50 mm) NC.

Table 3
Compressive cube test results.

Test	UHPC	NC
Compressive 2-in. (50 mm) cube test	24.8 ksi (171 Mpa)	7.62 ksi (52.55 Mpa)
Modulus of elasticity of 2-in. (50 mm) cube test	7850 ksi (54.14 Gpa)	3417 ksi (23.6 Gpa)
Compressive 3-in. (75 mm) cube test	19.4 ksi (133.8 Mpa)	9.4 ksi (64.8 Mpa)
Modulus of elasticity 3-in. (75 mm) cube test	7400 ksi (51 Gpa)	3461 ksi (23.8 Gpa)

(500 × 150 × 150 mm) with a span of 18 in. (450 mm) were used for this test (see Fig. 6). The prisms were placed on the roller supports with the vertical molded faces located as the compression and tension faces. To ensure low horizontal forces due to support friction, the specimens were supported by steel rollers. The load was then applied via the hydraulically controlled constant load rate (29 lb/s) at the middle length through failure.

This method of testing is based on simple beam bending theory and linear elastic stress-strain behavior up to failure. Due to the nonlinear behavior of concrete, the assumption of a linear stress distribution is not valid; therefore, results obtained using this method are always greater than the direct tensile strength. Fig. 6 also shows pictures of typical UHPC and NC beams before and after testing. Notice that in the case of UHPC, the beam remains intact due to the presence of the fibers, while NC prisms failed in brittle behavior. The average result of the tensile strength from the flexural test of UHPC and normal concrete were 3.17 ksi (21.9 Mpa) and 0.7 ksi (4.9 Mpa) respectively. The load-displacement curve for both materials obtained from flexural tests is shown in Fig. 7.

As shown, the UHPC prism's deflection increased linearly until the initiation of initial crack and was proportioned to the load. After the first crack, deflection increased nonlinearly until the ultimate was reached. UHPC showed 4.5 times higher flexural strength compared to NC. The ductile behavior of UHPC compared to NC also can be seen in the curves.

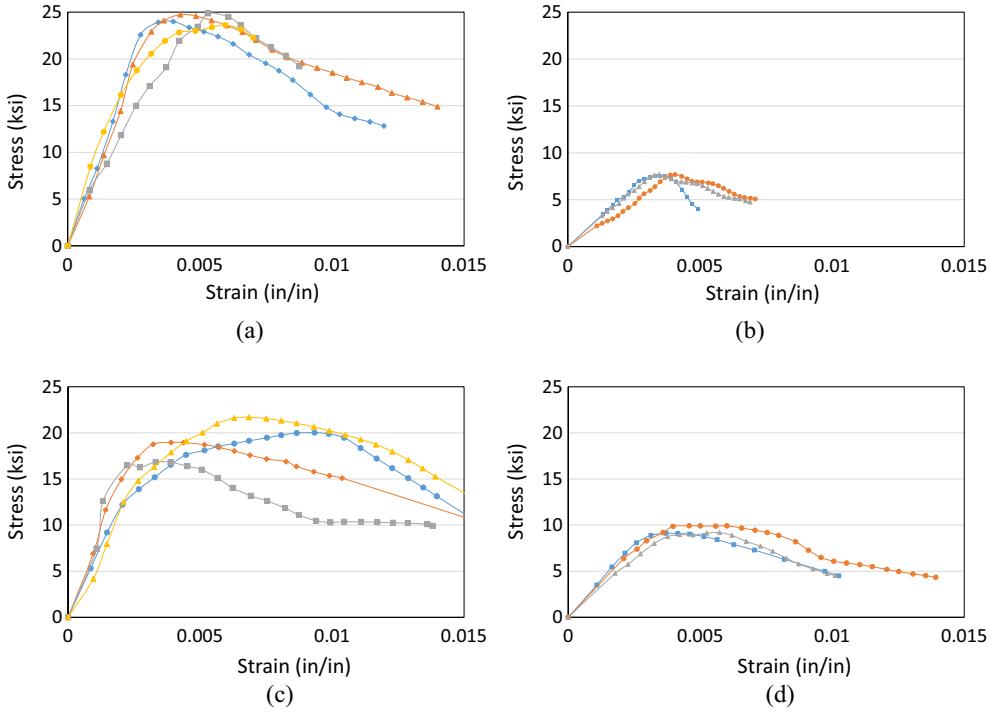

Fig. 5. The stress-strain curve based on cubic test of the specimens: a) UHPC 2 in. (50 mm), b) NC 2 in. (50 mm), c) UHPC 3 in. (75 mm), and d) NC 3 in. (75 mm).

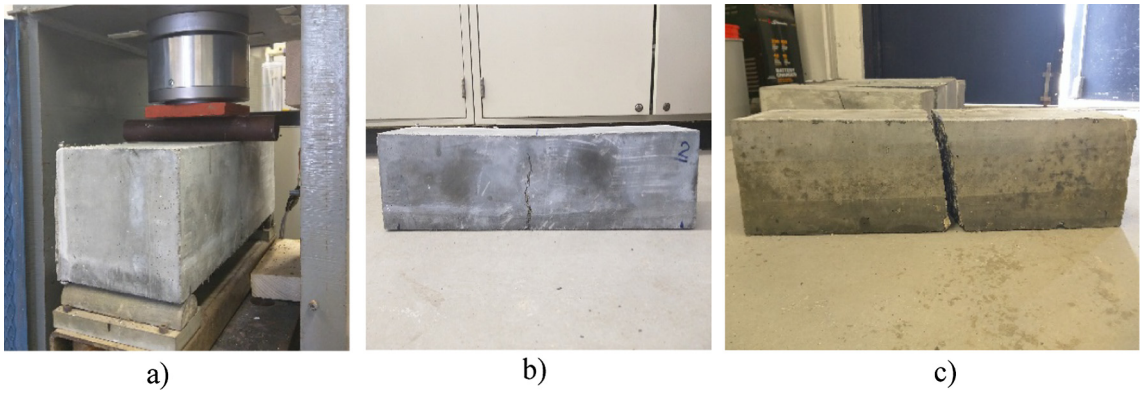

Fig. 6. a) UHPC prisms before test, b) UHPC prisms after test, and c) NC prisms after test.

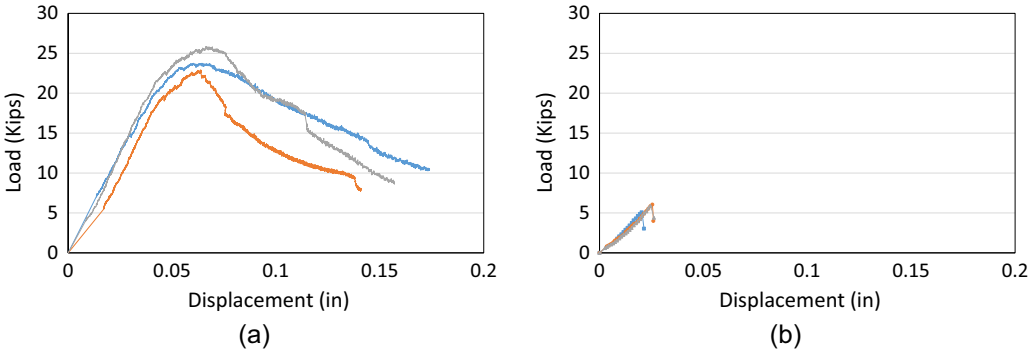

Fig. 7. The load-displacement curve for beam test of the specimens: a) UHPC, and b) NC.

3.2.2.2. Direct tensile test. The direct tensile test is a uniaxial test in which the tensile strength of a mortar is determined by pulling the specimen apart. AASHTO T132 [17], describes a test method called briquette tension test method, involving a direct tension testing of a small cement mortar briquette. The dog-bone shaped briquette has a 3-in. (75 mm) length, 1-in. (25 mm) thickness, with a 1-in.^{2} (625 mm^2) cross section at mid-length. Since this method is recommended for cement mortar specimens, it cannot be an extremely reliable method for the normal concrete with coarse aggregates. However, due to a comparison of materials behavior in this study, the direct tensile test was done for NC as well. In addition, in the case of UHPC as the composition shows the aggregate size of UHPC will not be an issue; however, due to the small cross-section of the briquette, fibers will not be randomly distributed as is preferred.

In AASHTO T132 [17], the loading rate is recommended at 600 lb/min. This portion of the test method was modified, and the tests were conducted at a displacement rate of 0.001 in./s (0.025 mm/s) suggested by Graybeal [18].

Fig. 8 shows typical UHPC and NC briquettes before and after testing. As shown, the steel fibers bridge the crack at the middle. As the fibers pull out of the matrix across the crack, the load capacity decreases until the total strength loss, while NC briquettes took apart suddenly after reaching the peak load. The average results of the tensile strength from briquettes for UHPC and regular concrete were 1.3 ksi (9 Mpa) and 0.51 ksi (3.5 Mpa) respectively.

Fig. 9 presents the load-displacement that resulted for each concrete type. The results indicate that UHPC behaved linear-elastically up to first cracking, followed by a significant amount of post-cracking load-carrying capacity. This is explained by the presence of the composite action of the fibers that bridges across the cracks. On the contrary, the NC briquettes failed briskly owning with the localization of the maximum strain in a single crack (Fig. 10).

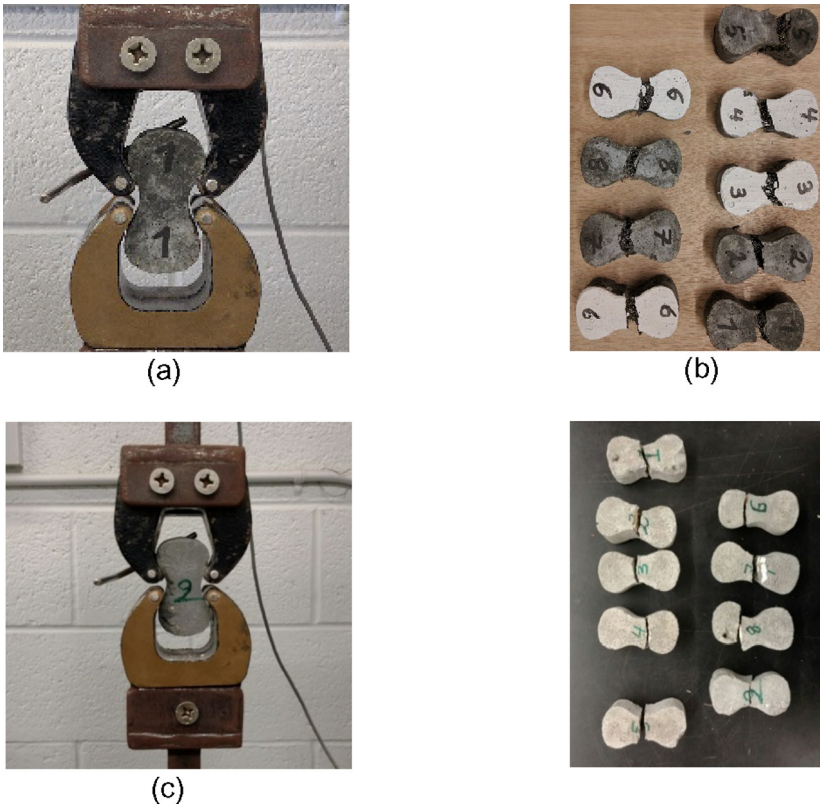

Fig. 8. a) UHPC briquette before test, b) UHPC briquettes after test, c) NC briquette before test, and d) NC briquettes after test.

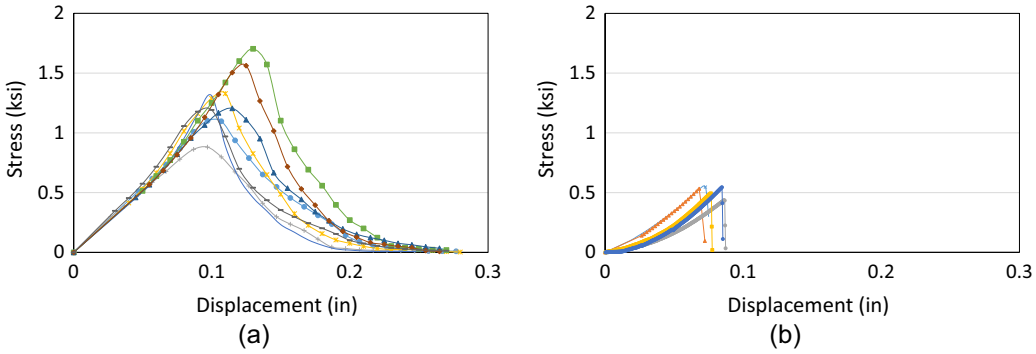

Fig. 9. The Stress-displacement curves of the briquette specimens: a) UHPC, and b) NC.

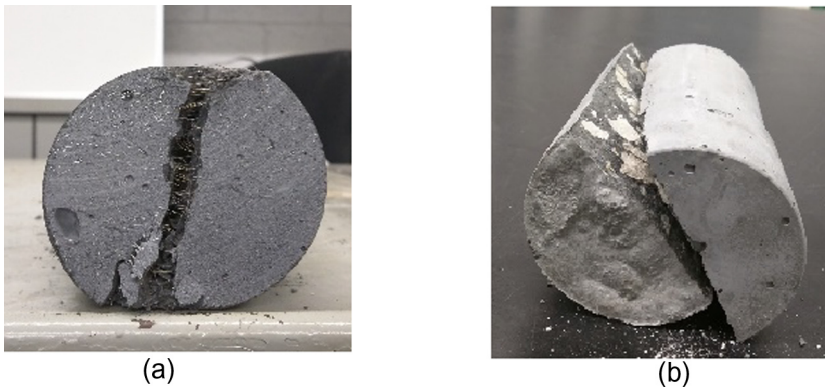

Fig. 10. a) UHPC splitting cylinder after test, and b) NC splitting cylinder after test.

3.2.2.3. Splitting tension. In the splitting tension test method, a cylindrical or cubical test specimen is located on its side under compression loading until it splits into two pieces lengthwise when its tensile strength is reached. Therefore, the peak load carried by the specimen is used to determine the splitting tensile strength. This test is increasingly popular as it can be more easily run. It was commonly known as the "Brazilian Method" in the 1970's and is currently cited by ASTM C 496, "Splitting Tensile Strength of Cylindrical Concrete Specimens" [15].

This test used 3-in. diameter cylinders. The load rate for these tests was set at 210 lb/s. Although this method is commonly completed on brittle concrete where a complete failure occurs with a single crack, again in order to compare the material behavior of NC and UHPC it has been done for both NC and UHPC. The reason that this method is not reliable for fiber-reinforced concrete can be explained due to the different behavior of ductile materials, particularly UHPC. In these concretes, fibers enable the specimen to carry the load after the failure that has already taken place.

In the case of UHPC, the results show significant compressive crushing arises at the platens of the testing machine owning with the steel fiber content. It also is noticeable that the UHPC cylinders did not split into two pieces, and that is due to the presence of fibers. The average result of the tensile strength from splitting test for UHPC and regular concrete were 3 ksi (20.7 Mpa) and 0.48 ksi (3.5 Mpa) respectively.

In this study, the splitting tensile strength of UHPC was determined as the first point in which the load carrying instability take place by crack initiation, and further load carried by the specimen after crack initiation was recognized more related to toughness than the actual increase in tensile strength of the material. The results of splitting test are illustrated in Fig. 11.

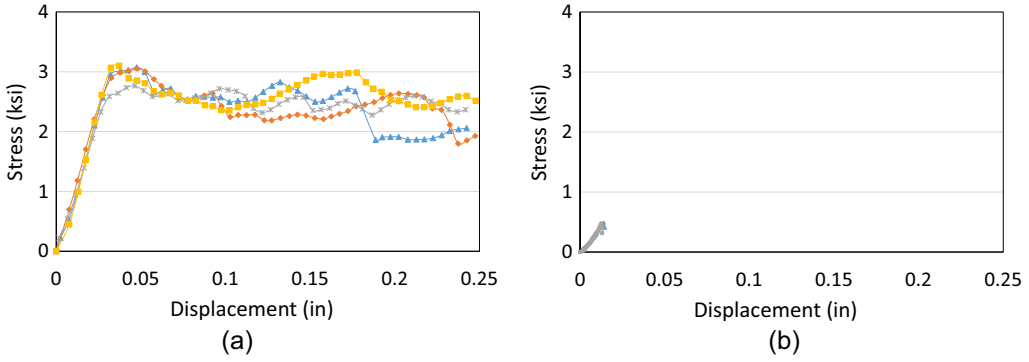

Fig. 11. The stress-displacement curve: a) UHPC, and b) NC.

Frequently, the tensile strength of concrete is defined as a percent of the compressive strength. The results from flexural prisms, briquette, and splitting tensile tests have been normalized by the 28-day compressive strength of cylinders.

3.3. Experimental result discussion

Experimental results show that among the two considered material, UHPC had a significant improved performance compared to normal strength concrete. In general, the compressive and tensile strength, ductility and modulus of elasticity of UHPC were notably higher than normal strength concrete. The mode of failure and behavior of UHPC test specimens after peak load exhibit the influence of fibers For UHPC, the compressive strength was similar for the cube (3 in.) and cylinder specimens (3 × 6 in.) while the cube (2 in.) specimen exhibited higher ultimate strength. Fig. 12 displays the average compression and tensile strength of tested UHPC compared with normal concrete.

4. Numerical study

This section presents the numerical study of UHPC behavior and failure. The simulation of UHPC material through commercial FE software allows for the study of the structures including UHPC. A three-dimensional FEM simulation is used to model the failure process of the experimentally tested compression cylinders and cubes along with flexural prisms. The commercial software Abaqus is commonly utilized in research, and the concrete plasticity damage (CDP) model in this software can predict the behavior of the concrete with reasonable accuracy. This model has been employed by researchers to model conventional concrete [19]. In this study, the CDP model was used to simulate UHPC, and the mechanical behavior obtained through experiment is transferred to the numerical model.

The concrete material parameters used in this study are the modulus of elasticity (E), Poisson's ratio (v), and the CDP parameters. In the CDP, for cracked concrete, a constant value for Poisson's ratio is considered. The primary values of the CDP parameters include dilation angle (ψ), shape factor (Kc), stress ratio σb0/σc0, eccentricity, and viscosity parameter. In the current study, the value of all parameters and modeling technique were based on previous studies done by other researchers [19–22] then calibrated with the experimental results obtained through tests. Table 2 presents all the parameters for CDP modeling.

The influence of mesh size on the accuracy of the numerical simulation has been investigated with three different sizes of mesh including 0.5 in. (12.5 mm), 1 in. (25 mm), and 1.5 in. (37.5 mm). Due to the uncertainty in boundary condition, such as grip slippage in briquette tensile test and different behavior of fiber reinforced concrete in splitting tensile test, these tests have not been included in the FEM. The friction of boundary condition has not been considered in simulation, and the loading of all models was displacement control (Table 4).

Figs. 13–16 show the Abaqus FE predictions with different mesh size for each group of specimens compared with the results of laboratory experiments, which closely follow the test data.

Although there is good agreement between the laboratory tests and numerical models, the slight difference in performance can be explained by the difference in boundary condition of the experimental specimen and the FE model, for example, the amount of friction between the loading plates and the specimens are not considered in FE modeling. Most importantly, in modeling the effort was to define one single material to have good agreement with the experimental data for all test specimens. Therefore, it was not possible to fit all results completely. It is worth to mention that there are many parameters that can affect the results of the test results including the amount of fibers, the age of the concrete, etc. The influence of each parameter will be considered for future studies.

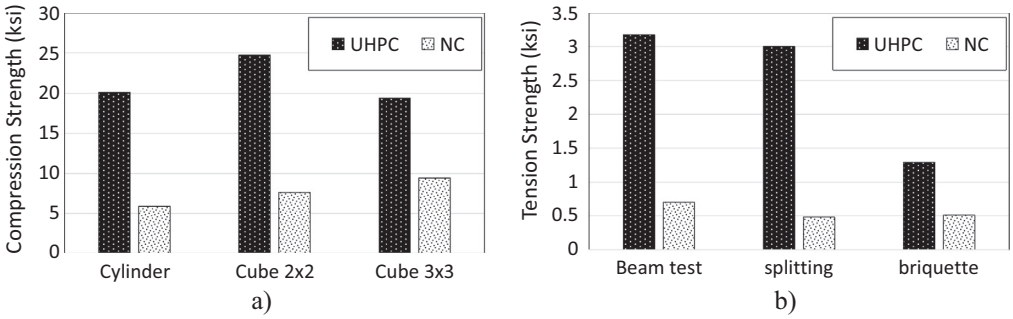

Fig. 12. Average compression and tensile strength of tested UHPC compared with normal concrete a) Compression strength and b) Tension strength.

Table 4
The employed material parameters for the FE computation which set according to the results of the experimental results (units:ksi).

Elastic Parameter					
Young's Modulus	7500 ksi (54710 Mpa)	Poisson's Ratio		0.18	
Concrete Damage Plasticity (CDP) Parameters					
Plasticity		Compressive Behavior		Tensile Behavior	
Dilation Angle	56	Yield Stress	Inelastic Strain	Yield Stress	Cracking Strain
Eccentricity	0.1	18 ksi (124 Mpa)	0	0.1 ksi (0.7 Mpa)	0
fb0/fc0	1.1	20 ksi (138 Mpa)	0.001	1.4 ksi (9.7 Mpa)	0.0035
k	0.66	11 ksi (76 Mpa)	0.009	0.3 ksi (2.1 Mpa)	0.05
Viscosity Parameter	0				
Mesh Type: C3D20R (A 20-node Quadratic brick, reduced integration)					

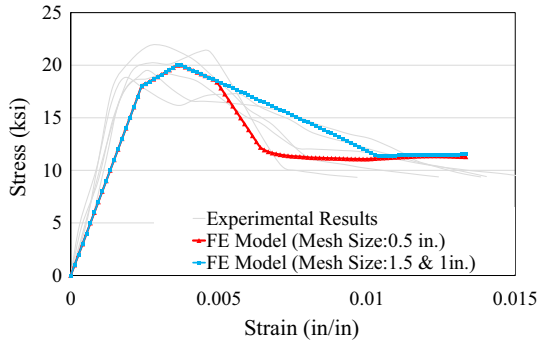

Fig. 13. UHPC cylinder compression test results compared with numerical result.

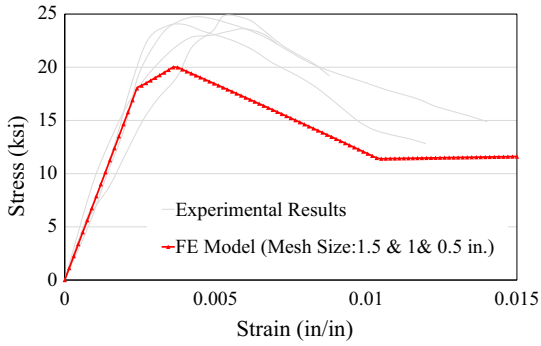

Fig. 14. UHPC 2 in. (50 mm) cubic compression test results compared with numerical result.

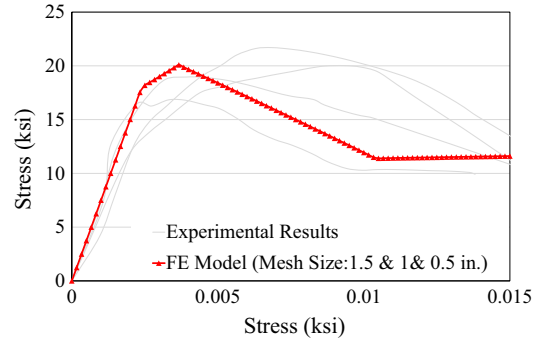

Fig. 15. UHPC 3 in. (75 mm) cubic compression test results compared with numerical result.

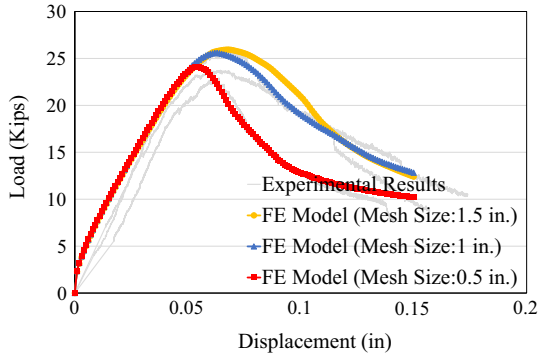

Fig. 16. UHPC flexural strength test results compared with numerical result.

5. Conclusion

To determine the basic behaviors of UHPC and NC, experimental tests have been done on the materials including cylinder, and cube compressive strength (2 × 2- and 3 × 3-in.) tests, as well as three-point flexural strength, briquette tensile, and splitting tension test.

Results obtained from the experimental phase of the study indicate that the compressive strength of commercial UHPC, used in this study, was three to four times greater than normal strength concrete. Moreover, higher modulus of elasticity (approximately two times) of UHPC specimens was obtained compared with the NC. The strong mechanical interlocking force between steel fibers and concrete matrix cylinders and cubes remained intact even after failure loading, whereas the control sample of normal strength concrete after failure split into large concrete pieces. Consequently, UHPC can foster high compressive strength without scarifying the ductility.

Furthermore, in the case of UHPC specimens, a higher tensile strength and ductility of the material compared to regular concrete was observed (two to four times greater). This is a result from a strong interlocking force between fibers and concrete matrix after the ultimate tensile capacity. Briefly, the results demonstrate the superior material properties of UHPC, particularly compared to regular concrete in both compression and tension.

The numerical analysis provides the mechanical properties of UHPC that can be used in FE software using CDP to define Ductal UHPC in the absence of sufficient experimental data. As shown in the result, employed material parameters for the FE model can provide the researchers a reliable prediction with good accuracy, which can be used in their projects as primary data.

References

[1] Henry G. Russell, Benjamin A. Graybeal, Ultra-High Performance Concrete: A State-Of-The-Art Report for the Bridge Community, No. FHWA-HRT-13-060, 2013.
[2] Benjamin Graybeal, Ultra High Performance Concrete FHWA-HRT-11-038 (2011).
[3] Pierre Richard, Marcel Cheyrezy, Composition of reactive powder concretes, Cem. Concr. Res. 25 (7) (1995) 1501–1511.
[4] Byung Hwan Oh, Flexural analysis of reinforced concrete beams containing steel fibers, J. Struct. Eng. 118 (10) (1992) 2821–2835.
[5] Samir A. Ashour, Faisal F. Wafa, Flexural behavior of high-strength fiber reinforced concrete beams, Struct. J. 90 (3) (1993) 279–287.
[6] Giuseppe Campione, Maria Letizia Mangiavillano, Fibrous reinforced concrete beams in flexure: experimental investigation, analytical modelling and design considerations., Eng. Struct. 30 (11) (2008) 2970–2980.
[7] D.H. Lim, B.H. Oh, Experimental and theoretical investigation on the shear of steel fibre reinforced concrete beams, Eng. Struct. 21 (10) (1999) 937–944.
[8] Kay Wille, Antoine E. Naaman, Gustavo J. Parra-Montesinos, Ultra-High Performance Concrete with compressive strength exceeding 150 MPa (22 ksi): a simpler way, ACI Mater. J. 108 (1) (2011).
[9] Srinivas Allena, Craig M. Newtson, Ultra-high strength concrete mixtures using local materials, J. Civil Eng. Arch. 5 (4) (2011).
[10] A.S. Dili, Manu Santhanam, Investigations on reactive powder concrete: a developing ultra high-strength technology, Indian Concr. J. 78 (4) (2004) 33–38.
[11] Benjamin A. Graybeal, Material Property Characterization of Ultra-High Performance Concrete, No. FHWA-HRT-06-103, 2006.
[12] Benjamin A. Graybeal, Flexural behavior of an ultrahigh-performance concrete I-girder, J. Bridge Eng. 13 (6) (2008) 602–610.
[13] Henry G. Russell, Benjamin A. Graybeal, Ultra-High Performance Concrete: A State-Of-The-Art Report for the Bridge Community, No. FHWA-HRT-13-060, 2013.
[14] Mohamadtaqi Baqersad, Ehsan Amir Sayyafi, Hamid Mortazavi Bak, State of the art: mechanical properties of ultra-high performance concrete, Civ. Eng. J. 3 (3) (2017) 190–198.
[15] ASTM International, Annual Book of ASTM Standards, ASTM, West Conshohocken, PA, 2012.
[16] Yeonho Park, Ali Abolmaali, Young Hoon Kim, Masoud Ghahremannejad, Compressive strength of fly ash-based geopolymer concrete with crumb rubber partially replacing sand, Constr. Build. Mater. 118 (2016) 43–51.
[17] AASHTO T132, Standard Method of Test for Tensile Strength of Hydraulic Cement Mortars, In America Association of State Highway and Transportation Officials, Standard Specifications for Transportation Materials and Methods of Sampling and Testing, Washington, DC, 2000.

[18] Benjamin Allen Graybeal, Characterization of the behavior of ultra-high performance concrete. Diss. 2005.
[19] Tomasz Jankowiak, Tomasz Lodygowski, Identification of parameters of concrete damage plasticity constitutive model, Found. Civil Environ. Eng. 6 (1) (2005) 53–69.
[20] Linfeng Chen, Benjamin A. Graybeal, Finite Element Analysis of Ultra-High Performance Concrete: Modeling Structural Performance of An AASHTO Type II Girder and a 2nd Generation Pi-Girder, No. FHWA-HRT-11-020, 2010.
[21] Somaye Fakharian Qom, Yan Xiao, Mohammed Hadi, Evaluation of Cooperative Adaptive Cruise Control (CACC) Vehicles on Managed Lanes Utilizing Macroscopic and Mesoscopic Simulation, in: Transportation Research Board 95th Annual Meeting, No. 16-6384, 2016.
[22] Jay Shen et al., Seismic performance of concentrically braced frames with and without brace buckling, Eng. Struct. 141 (2017) 461–481.